Nanodot-Cavity Electrodynamics and Photon Entanglement

Wang Yao, Renbao Liu, and L. J. Sham

Department of Physics, University of California–San Diego, La Jolla, California 92093-0319, USA

(Received 10 December 2003; published 27 May 2004)

Quantum electrodynamics of excitons in a cavity is shown to be relevant to quantum operations. We present a theory of an integrable solid-state quantum controlled-phase gate for generating entanglement of two photons using a coupled nanodot-microcavity-fiber structure. A conditional phase shift of $O(\pi/10)$ is calculated to be the consequence of the giant optical nonlinearity keyed by the excitons in the cavities. Structural design and active control, such as electromagnetically induced transparency and pulse shaping, optimize the quantum efficiency of the gate operation.

DOI: 10.1103/PhysRevLett.92.217402 PACS numbers: 78.67.Hc, 03.67.Mn, 42.50.Hz, 42.50.Pq

The semiconductor nanodot plays a key role in nanoscience as has been demonstrated by the electrical control of transport [1] and the optical control of quantum operations [2]. Following the study of quantum electrodynamics of atoms in cavity (CQED) [3,4], an effort is under way in the study of CQED of excitons in nanodots [5]. We report here the results of a theoretical study of excitons in CQED as illustrated by the proposal of a solid-state controlled-phase gate which entangles two photons.

Entangled photon pairs are the mainstay of quantum information processing [6] and the controlled gate which conditions the dynamics of one photon on the state of the other also enables a key logic operation for quantum computation. There are two approaches to realize such gates: (i) linear optics with projective measurements [7] and (ii) nonlinear optics at the discrete photon level. The logic gate working with few-photon nonlinear optics requires an impractical interaction length (e.g., several meters) in conventional Kerr media [8]. To obtain giant optical nonlinearity for a two-photon logic gate, novel schemes have been demonstrated, e.g., the atom-cavity QED [9], or proposed, e.g., slow light in a coherently prepared atomic gas exhibiting electromagnetically induced transparency (EIT) [10].

The relevance of excitons in CQED is strengthened by the recent advances in solid-state photonics and optoelectronics. We expect that the localization of the optical excitations would lead to ready integration of the solid-state cavity devices with extant devices. Advances relevant to our proposal in semiconductor quantum devices include single photon sources operating at room temperature [11,12], high-Q microspheres and their coupling to nanodots [5] and to fibers [13], and photonic lattice waveguides and cavities [14,15].

The qubit in our scheme is represented by two polarization states of a photon. In a quantum controlled-phase gate, a two-photon state acquires a phase-shift conditional to their polarization configuration. The arrangement of our proposed device is given in Fig. 1(a). Two photons traveling along two optical fibers receive their interaction by coupling to two silicon microsphere cavities which are joined by a doped nanodot. The dot provides in theory [16] a strong third-order optical nonlinearity which is essential for a controlled interaction between two photons. Two cavities of different resonant frequencies are needed to afford control of coupling to either photon. They also act as an *in situ* energy filter preventing two photons ending in the same fiber.

The photon scattering at the phase gate has inevitably some unwanted dynamics such as polarization-dependent reflection and motion-polarization entanglement. By relying on the transmission probability, the gate has the probabilistic nature as the linear optics procedure. The essential distinction lies in our use of the strong nonlinearity to provide definite interaction dynamics in the cavities versus the entanglement generated by the projective measurement. The probabilistic nature arises from the

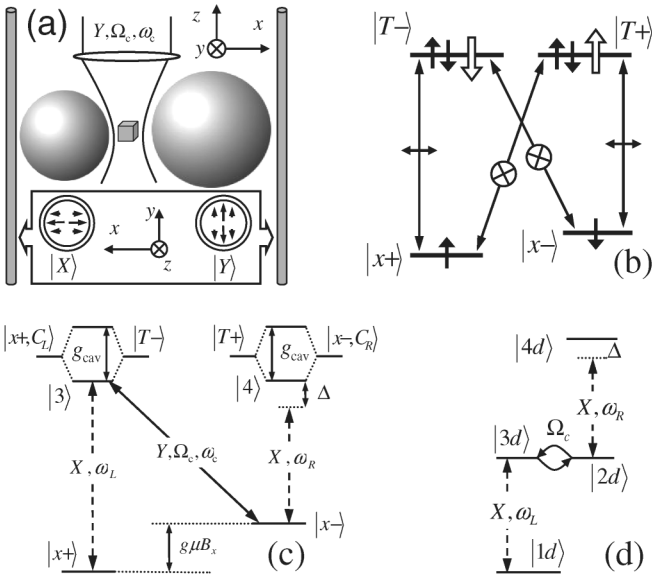

FIG. 1. The coupled system of fibers, cavities, and nanodot: (a) the physical structure, (b) the selection rules for the electron-trion transitions, (c) the energy structure, and (d) the dressed energy states. See the text for an explanation.

 0031-9007/04/92(21)/217402(4)$22.50

coupling of the photons to the solid-state system, which is unavoidable in any system, but its effect can be ameliorated. Our solution is two pronged: to eliminate the linear reflection by EIT and to minimize motion-polarization entanglement by pulse shaping and system design.

The two LP_{11} modes in a step index optical fiber [17] are chosen as the two polarization states $|X\rangle$ and $|Y\rangle$ for the qubits [see Fig. 1(a)]. The relevant modes in the microcavities are chosen to be the TE modes resonant with the nanodot transitions while the other TE modes and all TM modes are tuned far off resonant for a small cavity ($\sim\mu$m) [18]. The TE cavity mode can be excited only by an $|X\rangle$ photon in the fiber, whose coupling strength to the cavity on the left (right), $\kappa_{L(R)}$, is designed by adjusting the distance between the cavity and the fiber [13]. Thus, only in the $|XX\rangle$ state do the two incoming photons interact via the cavity-dot coupling system, resulting in a conditional phase shift.

The strong photon-photon interaction induced by the dot-coupled cavities is favored by both the small cavity-mode volume and the large dipole moment of the nanodot transitions, but the nanodot which contains a single active electron plays an essential role. The basic nonlinear optical process is illustrated with the aid of the energy structures in Fig. 1(c). A strong magnetic field is applied along the x direction to produce nondegenerate transitions from the electron spin states to the charged exciton states (trions), which are tuned, respectively, in resonance with the two cavity modes. The two split electron states are $|x\pm\rangle \equiv (1/\sqrt{2})(e_+^\dagger \pm e_-^\dagger)|G\rangle$, and the two degenerate trion states are $|T\pm\rangle \equiv (1/\sqrt{2})(e_+^\dagger e_-^\dagger h_-^\dagger \pm e_+^\dagger e_-^\dagger h_+^\dagger)|G\rangle$, where $e_\pm^\dagger$ and $h_\pm^\dagger$ create electron and hole spin states along the z axis. The transition selection rules are [see Fig. 1(b)] $|x\pm\rangle \leftrightarrow |T\mp\rangle$ via the X polarized field and $|x\pm\rangle \leftrightarrow |T\pm\rangle$ via the Y polarized field. The spatial configuration of the cavity-dot structure is such that the TE modes are X polarized at the site of the nanodot. The strong coupling between the trion state $|T-\rangle$ and the cavity-dot state $|x+, C_L\rangle$ (or between $|T+\rangle$ and the cavity-dot state $|x-, C_R\rangle$) mixes each pair into two split trion-polariton states, where $C_{L(R)}$ denotes the left (right) cavity mode. We denote the lower polariton states as $|3\rangle$ and $|4\rangle$, respectively. The four states, $|x+\rangle$, $|x-\rangle$, $|3\rangle$, and $|4\rangle$, form the level structure for the optical nonlinearity and all other states are assumed far off resonance. This situation is well satisfied by the cavity-dot coupling $g_{\rm cav} \sim 0.5$ meV, cavity decay rate into the fiber $\sim$0.1 meV, and Zeeman splitting $g\mu_B B_x \sim 1$ meV. The large value of $g_{\rm cav}$ is not critical provided that it is much larger than the cavity decay rate.

To induce an interaction between the photons from the left and right channels, a strong Y-polarized pump pulse is applied to resonantly couple the states $|x-\rangle$ and $|3\rangle$. Consider the effect of this classical field in the dressed basis: $|1d\rangle \equiv |x+\rangle|N\rangle$, $|3d\rangle \equiv |3\rangle|N\rangle$, $|2d\rangle \equiv |x-\rangle|N+1\rangle$, and $|4d\rangle \equiv |4\rangle|N+1\rangle$, where the Y-polarized coherent field is approximated by the Fock state $|N\rangle$ with large N. Figure 1(d) shows how the two X photons on separate fibers which affect separately the modes in the left and right cavities are coupled by the Y pump. The coupling strength Ω_c between $|3d\rangle$ and $|2d\rangle$ is proportional to the electric field strength. Thus, the nonlinear optical coupling is readily manipulated by switching on and off the pump pulse. The classical pump pulse also increases the efficiency of the operation by cooling the spin system and by eliminating the linear reflection and absorption by laser cooling and EIT [see Eq. (1a)] [10,19].

The transformation of the polarization state of two photons is carried out by scattering theory. The initial state is specified by the density matrix ρ_i in the basis set of the direct products of the polarization states, $|\sigma_L\sigma_R\rangle$ with $\sigma = X$ or Y, and of the wave vector states, $|k_L, k_R\rangle$. The transmitted state ρ_f is given by $t\rho_i t^\dagger$, where t is the transmission matrix. By design, t is diagonal in the polarization states. The final density matrix of the two-photon polarizations is obtained by tracing ρ_f over the wave vectors of the photons [20]. The transmission t is obtained via the T matrix conserving the total energy. The linear and nonlinear scattering terms are nonperturbatively calculated [21] as

$$T_{fi}^{(1)} = \delta_{\sigma_L,X}\delta_{k_R,k_R'}\frac{|\kappa_L|^2}{2}\frac{E_{1d}+\hbar ck_L-E_{2d}}{(E_{1d}+\hbar ck_L-E_{3d}+i\Gamma_3/2)(E_{1d}+\hbar ck_L-E_{2d})-\Omega_c^2}, \tag{1a}$$

$$T_{fi}^{(3)} = \frac{\delta_{\sigma_L,X}\kappa_L\Omega_c/\sqrt{2}}{(E_{1d}+\hbar ck_L-E_{3d}+i\Gamma_3/2)(E_{1d}+\hbar ck_L-E_{2d})-\Omega_c^2}\frac{\delta_{\sigma_R,X}|\kappa_R|^2/2}{E_{1d}+\hbar ck_L'+\hbar ck_R'-E_{4d}+i\Gamma_4/2} \times\frac{\delta_{\sigma_L,X}\kappa_L^*\Omega_c^*/\sqrt{2}}{(E_{1d}+\hbar ck_L'-E_{3d}+i\Gamma_3/2)(E_{1d}+\hbar ck_L'-E_{2d})-\Omega_c^2}, \tag{1b}$$

where $\Gamma_{3(4)}$ is the decay rate of the polariton states $|3\rangle$ (or $|4\rangle$). In silicon microspheres, the whispering gallery modes can have a Q factor as high as $\sim 10^8$ [5], so the intrinsic decay of the cavity modes can be neglected. The relaxation rate of trions is of the order of μeV, much less than the cavity-to-fiber loss. Thus, the decay of the trion polaritons is dominated by the leakage of the cavity modes into the fiber modes. The decay rates thus can be approximated as $\Gamma_{3(4)} \approx |\kappa_{L(R)}|^2/c$.

The Y-polarized photons are not scattered not being coupled to the cavities by design. The linear term in

Eq. (1a) contributes to the reflection of the X-polarized photon from the left channel. It is significantly suppressed by the EIT effect [19], which results from the destructive interference between the damped polariton state $|3d\rangle$ and the metastable state $|2d\rangle$ coupled by the classical pump field, as is evident from the vanishing of $T_{fi}^{(1)}$ when the incoming photon is in resonance with the $|1d\rangle \rightarrow |3d\rangle$ transition. The linear reflection of the X-polarized photons from the right channel is eliminated since the initial state of the system has been prepared in $|1d\rangle$ by the laser cooling cycle: The classical pulse pumps the ground state $|x-\rangle$ to $|3\rangle$, and then the polariton state relaxes to $|x+\rangle$ through the cavity-to-fiber leakage (details to be published). The reduction of the linear reflection in both fibers brings to prominence the third-order terms which are responsible for the gate operation. The nonlinear scattering term in Eq. (1b) is composed of three fractions corresponding to three processes: the excitation of the trion-polariton by the left-channel photon, the induced scattering of the right-channel photon, and the emission of the left-channel photon by the polariton recombination.

Because of the resonance features in the T matrix, the transmission coefficient $t_{XX} = fe^{-i\phi}$, where f and ϕ are functions of the wave vectors, can cause the amplitude and phase modulation of the transmitted wave since the incoming photons are in wave packets. The amplitude modulation can be suppressed by either using longer time pulses or working in the far-resonance region. Although often overlooked in phase-shift estimation based on $\chi^{(3)}$ susceptibility, the phase-variation effect results in distortion of the pulse shape and entanglement of the motion and polarization of the photons. The polarization states of the two photons are obtained by projection after the transmission. The effect of pulse deformation may be reduced by frequency filtering the transmitted pulse.

We show how shaping the input pulses leads to a reduction of the output pulse deformation. (i) As a consequence of the optical coupling between the $|3d\rangle$ and $|2d\rangle$ states, the choice of the left input photon to be within $\pm\Omega_c$ of being in resonance with the $|1d\rangle \rightarrow |3d\rangle$ transition, the linear reflection is reduced and the first factor on the right side of Eq. (1b) will yield a strong third-order transmission. (ii) To diminish the pulse distortion due to the sharp resonant structure around the $|2d\rangle \rightarrow |4d\rangle$ transition, the right-channel pulse is detuned about $\Gamma_4/2$ below the transition where the real part (corresponding to the phase shift) of $T^{(3)}$ is large and flat while the imaginary part (corresponding to the reflection) has decreased to a small value. (iii) To minimize the pulse broadening and distortion from the convolution of the input pulses with energy conservation, we choose the two input pulses to have square-shaped spectra with much different widths. In our design, $\Gamma_4/2$ is much larger than Ω_c, so the right-channel pulse is set the wider in frequency.

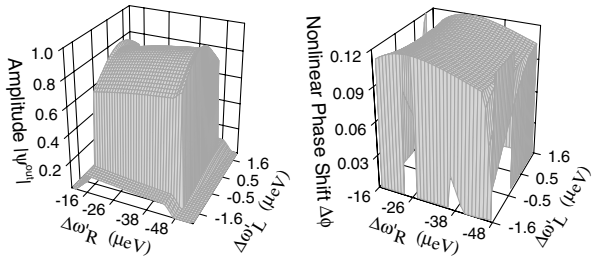

FIG. 2. The amplitude and phase of the transmitted two-photon wave function as functions of the detuning $\Delta\omega'_L \equiv \hbar ck'_L - (E_{3d} - E_{1d})$ and $\Delta\omega'_R \equiv \hbar ck'_R - (E_{4d} - E_{2d})$. The parameters are $\Gamma_3 = \Gamma_4 = 60$ μeV, $\Omega_c = 8$ μeV, and $g_{\rm cav} = 0.5$ meV. The input wave function is such that $\Psi^i(k_L, k_R) = \theta(48 + \Delta\omega_R)\theta(-16 - \Delta\omega_R)\theta(1.6 + \Delta\omega_L)\theta(1.6 - \Delta\omega_L)$ with arguments in units of μeV.

Figure 2 presents the transmitted wave function ($k'_L, k'_R > 0$) for incoming photons in square pulses with the polarization state $|XX\rangle$. Though visible, the pulse distortion and broadening and the inhomogeneity in the phase shift is quite small. A conditional phase shift of $\pi/29$ is obtained with a transmission probability of 0.72 and a 0.99 fidelity.

The loss in transmission and the pulse distortion in Fig. 2 result mainly from the imperfect EIT when the photon is off resonant with the $|1d\rangle \rightarrow |3d\rangle$ transition. Improvement of both the pulse shape and the transmission is effected by increasing the pump power Ω_c (in order to open a larger EIT window) and by using narrower bandwidth pulses at the expense of a weak nonlinear phase shift. An example is shown in Fig. 3, in which a nonlinear phase shift $\sim\pi/330$ is obtained almost without pulse-shape change or reflection loss, shown by the computed transmission probability of $\sim$0.982 and almost perfect fidelity.

The examples above show that reduction of the reflection and distortion of the photon pulses diminishes the gate phase and the entanglement. A small entanglement is still useful for some quantum information purposes [22]. Moreover, a large phase shift can be accumulated, by either passing a photon pair many times through the phase gate or using a series of many identical gates

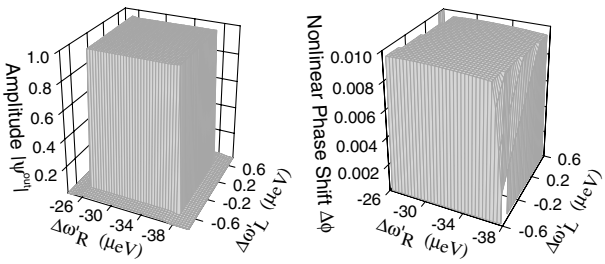

FIG. 3. The same as Fig. 2 except that the parameters are $\Gamma_3 = 45$ μeV, $\Gamma_4 = 60$ μeV, $\Omega_c = 15$ μeV, $g_{\rm cav} = 0.5$ meV, and $\Psi^i(k_L, k_R) = \theta(38 + \Delta\omega_R)\theta(-26 - \Delta\omega_R) \times \theta(0.6 + \Delta\omega_L)\theta(0.6 - \Delta\omega_L)$.

TABLE I. Operation efficiency of the symmetrical circuits composed of $n + n$ gates with parameters $\Gamma_3 = 0.06$ meV, $\Gamma_4 = 0.5$ meV, and $\Omega_c = 6.2$ μeV. The left- and right-channel Gaussian pulses with FWHM 7.5 and 50 μeV are resonant with the left and right polariton transitions, respectively. C denotes the concurrence and $E(C)$ the entanglement of formation.

n	Transmission	Fidelity	Purity	C	$E(C)$
2	0.1165	0.8638	0.9591	0.7277	0.6272
4	0.020 74	0.9758	0.9850	0.9515	0.9306

integrated into a single chip. With modern fabricating techniques, the integrated quantum gates can be constructed either with microdisks and waveguides etched on semiconductor heterostructures [23] or with point and line defects engineered in photonic lattices [14].

To use the system to produce an entangled photon pair rather than to perform a controlled-phase operation, we optimize the entanglement by a different procedure. The quantum operation is favored by maximizing the transmission, but the entanglement is favored by symmetrizing the two photons for maximal projection of the polarization degrees of freedom. First the input state is prepared as the equal linear combination of the four polarization states of the two photons. Then the state is passed n times through the coupled system as described above, undergoes single bit operation swapping the $|X\rangle$ and $|Y\rangle$ states in both photons, and is passed through the phase gate n more times. This symmetrizes the transmitted density matrix after projecting out the motional degrees of freedom. Table I shows the calculated results for $2 + 2$ and $4 + 4$ gates. The transmission probabilities T are much lower than for the phase operation. The quantitative measures of the operation including fidelity $\mathrm{Tr}[\rho_t \rho_{\mathrm{ideal}}]$ towards the maximally entangled state $(1/\sqrt{2})(|XY\rangle + |YX\rangle)$, the purity $\mathrm{Tr}[\rho_t^2]$, the concurrence C, and the entanglement of formation $E(C)$ [24] all show excellent entanglement.

In summary, we have proposed a solid-state controlled-phase gate for two photons. The flying qubits are conducted through fibers coupled to scattering centers composed of microcavities connected by a doped semiconductor nanodot. This allows a fiber implementation of quantum information processor. Calculated results show that the system is flexible as a phase gate as well as producing strong entanglement. The trions in the doped nanodot used for nonlinear interaction here can be replaced by other electronic systems, such as biexcitons in an undoped nanodot (results will be published elsewhere), states in nanoclusters, or even some strong transitions in rare-earth impurities, e.g., the $4d$-$5f$ transition in Er^{2+}. The microcavity may be microspheres or defects in photonic lattices. The structure has unique features, such as small size, integrability, and stability, useful for quantum information and for scalable quantum computing.

This work was supported by NSF DMR-0099572, by ARDA/ARO DAAD19-02-1-0183, and by QuIST/AFOSR F49620-01-1-0497. L. J. S. thanks Y. Fainman for helpful discussions.

[1] W. G. van der Wiel, S. De Franceschi, J. M. Elzerman, T. Fujisawa, S. Tarucha, and L. P. Kouwenhoven, Rev. Mod. Phys. **75**, 1 (2003).
[2] X. Li, Y. Wu, D. Steel, D. Gammon, T. H. Stievater, D. Katzer, D. S. Park, C. Piermarocchi, and L. J. Sham, Science **301**, 809 (2003).
[3] H. J. Kimble, in *Cavity Quantum Electrodynamics*, edited by P. R. Berman (Academic Press, Boston, 1994), pp. 203–267.
[4] H. J. Carmichael, L. Tian, W. Ren, and P. Alsing, in *Cavity Quantum Electrodynamics* (Ref. [3]), pp. 381–425.
[5] H. Wang, P. Palinginis, X. Fan, S. Lacey, and M. Lonergan, in *Proceedings of the Quantum Electronics and Laser Science Conference* (Optical Society of America, Washington, D.C., 2000).
[6] C. H. Bennett, D. P. DiVincenzo, J. A. Smolin, and W. K. Wootters, Phys. Rev. A **54**, 3824 (1996).
[7] E. Knill, R. Laflamme, and G. J. Milburn, Nature (London) **409**, 46 (2001).
[8] B. C. Sanders and G. J. Milburn, Phys. Rev. A **39**, 694 (1989).
[9] Q. A. Turchette, C. J. Hood, W. Lange, H. Mabuchi, and H. J. Kimble, Phys. Rev. Lett. **75**, 4710 (1995).
[10] M. D. Lukin and A. Imamoğlu, Phys. Rev. Lett. **84**, 1419 (2000).
[11] P. Michler, A. Imamoğlu, M. D. Mason, P. J. Carson, G. F. Strouse, and S. K. Buratto, Nature (London) **406**, 968 (2000).
[12] B. Lounis, H. A. Bechtel, D. Gerion, P. Alivisatos, and W. E. Moerner, Chem. Phys. Lett. **329**, 399 (2000).
[13] S. M. Spillane, T. J. Kippenberg, O. J. Painter, and K. J. Vahala, Phys. Rev. Lett. **91**, 043902 (2003).
[14] A. Scherer, O. Painter, J. Vuckovic, M. Loncar, and T. Yoshie, IEEE Trans. Nanotechnol. **1**, 4 (2002).
[15] L. Pang, W. Nakagawa, and Y. Fainman, Appl. Opt. **42**, 5450 (2003).
[16] W. Yao, H. Ajiki, and L. J. Sham (unpublished).
[17] G. Cancellieri, *Single-Mode Optical Fibres* (Pergamon Press, New York, 1991).
[18] R. E. Benner, P. W. Barber, J. F. Owen, and R. K. Chang, Phys. Rev. Lett. **44**, 475 (1980).
[19] H. Schmidt and A. Imamoğlu, Opt. Lett. **21**, 1936 (1996).
[20] N. F. Mott and H. S. Massey, *The Theory of Atomic Collisions* (Oxford University Press, London, 1965).
[21] C. Cohen-Tannoudji, J. Dupont-Roc, and G. Grynberg, *Atom-Photon Interactions* (Wiley Interscience, New York, 1992).
[22] J. I. Cirac, W. Dür, B. Kraus, and M. Lewenstein, Phys. Rev. Lett. **86**, 544 (2001).
[23] S. C. Hagness, S. T. Ho, and A. Taflove, J. Lightwave Technol. **15**, 2154 (1997).
[24] W. K. Wootters, Phys. Rev. Lett. **80**, 2245 (1998).